Iranian Journal of Numerical Analysis and Optimization
Vol. 16, No. 2, 2026, pp 683–702
https://doi.org/10.22067/ijnao.2026.94933.1707
https://ijnao.um.ac.ir/

Research Article

Synchronization and control of discrete incommensurate fractional-order and variable-order neural networks

S. Momani, I.M. Batiha*, A. Hioual and A. Ouannas

Abstract

The examination of dynamics and synchronization within discrete fractional neural networks has attracted notable interest in contemporary studies. Nevertheless, current research has primarily focused on commensurate discrete fractional-order neural networks. This study aims to

*Corresponding author

Received 15 August 2025; revised 19 December 2025; accepted 13 January 2026

Shaher Momani
Department of Mathematics, Faculty of Science, University of Jordan, Amman 11942, Jordan. Nonlinear Dynamics Research Center (NDRC), Ajman University, Ajman, UAE. e-mail: s.momani@ju.edu.jo

Iqbal M. Batiha
Nonlinear Dynamics Research Center (NDRC), Ajman University, Ajman, UAE.
Department of Mathematics, Al Zaytoonah University of Jordan, Amman 11733, Jordan. e-mail: i.batiha@zuj.edu.jo

Amel Hioual
Laboratory of Dynamical Systems and Control, University of Oum EL-Bouaghi, Oum El Bouaghi 04000, Algeria. e-mail: amelhioual4@gmail.com

Adel Ouannas
Department of Mathematics and Computer Science, University of Oum EL-Bouaghi, Oum El Bouaghi 04000, Algeria. e-mail: ouannas.adel@univ-oeb.dz

How to cite this article
Momani, S., Batiha, I.M., Hioual, A. and Ouannas, A., Synchronization and control of discrete incommensurate fractional-order and variable-order neural networks. *Iran. J. Numer. Anal. Optim.*, 2026; 16(2): 683-702. https://doi.org/10.22067/ijnao.2026.94933.1707

explore the synchronization of incommensurate discrete fractional neural networks, spanning both constant and variable orders. By employing linear feedback control techniques, we establish a satisfactory criterion to guarantee the synchronization of noncommensurate discrete fractional neural networks with constant orders. This condition is formulated in terms of linear matrix inequalities, offering a systematic approach to synchronization. Furthermore, under specific conditions, the Lyapunov functional is employed to analyze the synchronization of noncommensurate discrete fractional neural networks with variable orders. This synchronization condition is solely dependent on the system parameters, facilitating easy verification and implementation. In order to confirm the efficacy and practicality of the proposed methodologies, two numerical examples are selected and presented, demonstrating the successful synchronization of incommensurate discrete fractional neural networks.

AMS subject classifications (2020): Primary 39A12; Secondary 34D06, 34D20, 92B20, 93C55, 39A30.

Keywords: Discrete incommensurate fractional neural networks; Discrete incommensurate variable-order neural networks; Lyapunov functional; Complete synchronization.

1 Introduction

In recent years, the analysis of nonlinear dynamical systems has increasingly focused on synchronization phenomena, owing to their fundamental role in science and engineering applications such as secure communications, signal processing, neural computation, and coordinated control of complex networks. With the widespread use of digital devices and numerical platforms, discrete-time models have become particularly relevant, as they naturally arise in digital circuits, computer simulations, and networked control implementations. Consequently, the synchronization and control of discrete-time chaotic systems has emerged as an active research area, especially when memory effects and long-term dependencies are taken into account.

To accurately capture such memory effects, fractional-order modeling has been widely adopted. Fractional-order systems generalize classical integer-order models by introducing nonlocal operators that depend on the entire past evolution of the system. In the discrete-time setting, fractional difference operators provide a flexible mathematical framework for modeling systems with hereditary properties. Foundational developments in discrete fractional calculus, including Riemann-type and nabla-type fractional differences and their associated transforms, have been established in works such as [2, 12]. More recently, stability and asymptotic behavior of incommensurate nabla fractional difference systems have been investigated in [7], while nonlinear nabla variable-order fractional discrete systems and their applications to neural networks were studied in [13]. These results form the mathematical basis for the analysis of fractional discrete neural networks.

Within this framework, a wide range of synchronization and control strategies has been proposed for discrete fractional-order chaotic systems. Active control techniques, which rely on real-time state reconstruction, have been successfully applied to achieve synchronization and secure communication in fractional-order discrete-time chaotic systems [8]. Impulsive control methods, based on intermittent control actions, were developed in [23] to synchronize fractional-order discrete chaotic systems with reduced control effort. Adaptive and sliding-mode-based strategies have also been investigated to improve robustness and precision, as demonstrated in fractional-order discrete-time synchronization problems arising in engineering applications [20]. In addition, linear state error feedback control remains a simple and effective approach for synchronizing chaotic discrete dynamical systems [36].

The incorporation of fractional difference operators into neural network models has revealed a rich variety of dynamical behaviors in discrete-time systems. Fractional-order discrete neural networks are capable of exhibiting chaos, bifurcations, multistability, and complex attractors, which are not observed in their integer-order counterparts. Chaos generation and applications to image encryption were explored in fractional-order discrete neural networks in [5], while incommensurate fractional discrete neural networks with complex chaotic behavior were studied in [1]. The dynamics of fractional-order neural networks with discrete and distributed delays were investigated in [33]. Moreover, extensive research has been devoted to the stability and control of fractional discrete neural networks, including new stability criteria [17], solvability and stability of variable-order fractional discrete neural networks [16, 3], stabilization and synchronization of nonlinear fractional discrete neural networks [15], finite-time stability results for variable-order fractional difference equations [11], and finite-time stability analysis of various types of fractional discrete neural networks [14, 24].

Among the many dynamical phenomena observed in fractional neural networks, synchronization plays a particularly important role. Synchronization enables coordinated behavior between coupled neural systems and is essential for applications in information transmission and secure communications. Synchronization of fractional-order discrete-time neural networks with time delays has been studied in [10], while complete synchronization of discrete-time fractional-order coupled neural networks was analyzed in [6]. Global Mittag–Leffler stability and synchronization of complex-valued discrete-time fractional-order neural networks were investigated in [37], and finite-time synchronization of fractional-order memristive recurrent neural networks was reported in [21]. More refined synchronization patterns have also been explored, including synchronization analysis for discrete fractional-order complex-valued neural networks [22], quasi-projective synchronization of discrete-time fractional-order quaternion-valued neural networks [38], and lag synchronization of discrete fractional-order neural networks with time delays [10].

Despite these advances, much of the existing literature has focused on commensurate fractional-order systems, where all state variables share the same fractional order. However, in many realistic neural and biological systems, different neurons may possess distinct memory characteristics, leading naturally to incommensurate fractional-order models. In recent years, synchronization of incommensurate fractional-order neural networks has therefore attracted increasing attention. Predefined-time synchronization of incommensurate fractional-order competitive neural networks with time-varying delays was studied in [35]. Synchronization in incommensurate Riemann–Liouville fractional-order competitive neural networks with different time scales was investigated in [9]. Lag quasi-synchronization of incommensurate fractional-order memristor-based neural networks with nonidentical characteristics was addressed in [18], while a detailed dynamical analysis and digital circuit realization of incommensurate fractional-order Hopfield neural networks was presented in [34].

In parallel, variable-order fractional models have emerged as a powerful generalization of constant-order fractional systems, allowing the fractional order to vary with time and thereby providing a more accurate description of evolving memory effects. Variable-order fractional discrete neural networks have been analyzed in terms of existence, uniqueness, stability, and finite-time behavior in [16, 3, 11, 14]. These models further enrich the dynamics of neural networks and pose new challenges for synchronization and control design.

It is also worth noting that synchronization of chaotic and fractional-order systems has been extensively studied through generalized, hybrid, and projective synchronization frameworks. Comprehensive treatments of fractional-order control and synchronization can be found in the monograph [4]. Robust and hybrid synchronization methods for fractional and integer-order chaotic systems were developed in [26, 25, 27, 29], while generalized synchronization of discrete-time chaotic systems with different dimensions was investigated in [32]. Fractional-order discrete-time chaotic systems exhibiting chaos, stabilization, and synchronization were studied in [19], and chaos control and synchronization of fractional discrete-time systems with no equilibrium were reported in [31]. Applications of chaotic synchronization to secure communication schemes were further explored in [30], and inverse full-state hybrid function projective synchronization was investigated in [28]. These works provide an important theoretical and methodological foundation for the present study.

Motivated by the above discussion, this paper investigates the synchronization and control of discrete incommensurate fractional-order and variable-order neural networks. Using the Nabla Caputo fractional difference operator, we propose novel discrete neural network models that incorporate both heterogeneous (incommensurate) and time-varying (variable-order) memory effects. Simple linear control laws are designed to achieve synchronization between drive and response networks. By constructing suitable Lyapunov functionals, new sufficient conditions are derived to guarantee synchronization for both constant-order and variable-order incommensurate neural networks

The remainder of this paper is organized as follows. Section 2 introduces preliminary results from discrete fractional calculus and variable-order fractional difference theory based on the nabla operator. Section 3 presents synchronization criteria for discrete incommensurate fractional-order neural networks with constant orders. Section 4 extends the results to discrete incommensurate variable-order neural networks. Section 5 provides numerical simulations to validate the theoretical findings. Finally, section 6 concludes the paper and outlines directions for future research.

2 Preliminaries

In the following discussion, we introduce fundamental definitions and key principles concerning discrete fractional calculus to lay the foundation for our investigation. Consider real numbers a and b, along with a positive constant h. We utilize the notation $\mathbb{N}_a = \{a, a+1, a+2, \ldots\}$ to denote a set of natural numbers starting from a.

Definition 1. [2] For a function $x : \mathbb{N}_\theta \to \mathbb{R}$ with θ as the starting point, and for $\theta > 0$, the θth order summation operator is defined as follows:

$$ {}_a\nabla^{-\theta} x(t) = \frac{1}{\Gamma(\theta)} \sum_{s=a+1}^{t} (t-\rho(s))^{\theta-1} x(sh), \quad \rho(s) = s-1, \quad t \in \mathbb{N}_a. \tag{1} $$

Additionally, we establish the polynomial factorial function with ascending powers as

$$ t^{\theta} = \frac{\Gamma(t+\theta)}{\Gamma(t)}. $$

Definition 2. [2] Consider a function $x : \mathbb{N}_a \to \mathbb{R}$ defined on $\mathbb{N}_a$, where $\theta > 0$. The discrete Caputo nabla operator is expressed as

$$ {}_a^C\nabla^{\theta} x(t) = \frac{1}{\Gamma(1-\theta)} \sum_{s=a+1}^{t} (t-\rho(s))^{-\theta} \nabla x(s), \quad t \in \mathbb{N}_a. \tag{2} $$

Here,

$$ \nabla x(t) = x(t) - x(t-1). \tag{3} $$

Let the nonlinear incommensurate fractional-order discrete-time system be described by the nabla operator:

$$ {}^{C}_{a}\nabla^{\theta} x(t) = Ax(t), \tag{4} $$

where $\theta = (\theta_1, \theta_2, \ldots, \theta_n) \in (0, 1)$, $x(t) = (x_1(t), x_2(t), \ldots, x_n(t))$.

Theorem 2.1. [7] If $\det(I - HA) \neq 0$, then the system (4) possesses a unique solution for $x_0 \in \mathbb{R}^n$. Moreover, if all the eigenvalues of the characteristic equation expressed as

$$ \det\left(\operatorname{diag}\left(\left(1 - \frac{1}{s}\right)^{\theta_1}, \left(1 - \frac{1}{s}\right)^{\theta_2}, \ldots, \left(1 - \frac{1}{s}\right)^{\theta_n}\right) - \mathbf{A}\right) = 0 \tag{5} $$

reside within the unit disk, then the trivial solution of system (4) achieves asymptotic stability.

Lemma 2.1. Examine the subsequent fractional-order difference inequalities accompanied by initial conditions: $0 \leq V_i(0, x_i(0)) \leq W_i(0, y_i(0)), i = 1, 2, \ldots,,$

$$ \begin{aligned} {}^{C}_{a}\nabla^{\theta_1} V_1(t, x_1(t)) &\leq {}^{C}_{a}\nabla^{\theta_1} W_1(t, y_1(t)), \\ {}^{C}_{a}\nabla^{\theta_2} V_2(t, x_2(t)) &\leq {}^{C}_{a}\nabla^{\theta_2} W_2(t, y_2(t)), \\ &\vdots \\ {}^{C}_{a}\nabla^{\theta_n} V_n(t, x_n(t)) &\leq {}^{C}_{a}\nabla^{\theta_n} W_n(t, y_n(t)). \end{aligned} $$

The subsequent inequalities are valid:

$$ V_i(t, x_i(t)) \leq W_i(t, y_i(t)), \quad \text{for all } t > 0, \quad i = 1, 2, \ldots, n, \tag{6} $$

where $V_i(t, x_i(t))$ and $W_i(t, x_i(t)) : [0, \infty) \times \mathbb{N}_a \to [0, \infty)$.

Definition 3. [13] Let $0 < \theta(t) \leq 1$ for all $t \in \mathbb{N}a$. Suppose that we have a function $x : \mathbb{N}a \to \mathbb{R}$. We define the left nabla fractional sum of order $\theta(t)$ as follows:

$$ {}_{a}\nabla^{-\theta(t)} x(t) = \frac{1}{\Gamma(\theta(t))} \sum_{s=a+1}^{t} (t - \rho(s))^{\overline{\theta(t)-1}} x(s), \quad t \in \mathbb{N}_{a+1}. \tag{7} $$

Definition 4. [13] Given a function $x : \mathbb{N}_{a+1} \to \mathbb{R}$ with $0 < \theta(t) < 1$, the Caputo nabla discrete difference with variable-order is expressed by

$$ {}^{C}_{a}\nabla^{\theta(t)} x(t) = \frac{1}{\Gamma(1 - \theta(t))} \sum_{s=a+1}^{t} (t - \rho(s))^{\overline{-\theta(t)}} \nabla x(s), \quad t \in \mathbb{N}_{a+1}. \tag{8} $$

Lemma 2.2. [13] Let $x : \mathbb{N}_{a+1} \to \mathbb{R}$; then $x(t)$ fulfills the following inequality:

$$ {}_{a}^{C}\nabla^{\theta(t)} x^2(t) \leq 2x(t)2x(t)\, {}_{a}^{C}\nabla^{\theta(t)} x(t). \tag{9}$$

Let us explore the dynamical system described by the following nonlinear nabla noncommensurate discrete fractional equations:

$$ {}_{a}^{C}\nabla^{\theta_{\mathfrak{i}}(t)} x_{\mathfrak{i}}(t) = f_{\mathfrak{i}}(t, x_{\mathfrak{i}}(t)). \tag{10}$$

In the context of the nabla discrete-time fractional-order system, we consider $\theta(t) \in (0,1)$, $x(t) \in D \subset \mathbb{R}^n$ representing the state space that includes the equilibrium point $x_e = 0$. The variable t is an element of $\mathbb{N}_{a+1}$, where $a \in \mathbb{R}$, and the function $f : \mathbb{N}_{a+1} \times D \to \mathbb{R}^n$ adheres to the Lipschitz continuity condition.

Theorem 2.2. [13] If we consider the system (10) defined under the Caputo definition, then the conditions for asymptotic stability can be established through the existence of class K functions $\gamma_1, \gamma_2, \gamma_3$, parameters $\gamma \in (0, \min \theta_i(t))$, $p_{\mathfrak{i}} > 0$, and Lyapunov functions $V_i(t, x_{\mathfrak{i}}(t)) : \mathbb{N}_a \times D \to \mathbb{R}$ for each $\mathfrak{i} = 1, 2, \ldots, n$, satisfying

$$ \gamma_1(||x(t)||) \leq \sum_{i=1}^{n} p_i\, {}^{C}\nabla^{\theta_i(t)-\gamma} V_i(t, x_i(t)) \leq \gamma_2(\|x(t)\|), \tag{11}$$

$$ \sum_{i=1}^{n} p_i \frac{\partial V_i(t, x_i(t))}{\partial x_i(t)} f_i(t, x(t)) \leq -\gamma_3(\|x(t)\|). \tag{12}$$

In the context where $x(t) \in D$, $t \in \mathbb{N}_{a+1}$, $a \in \mathbb{R}$, and $V_i(t, x_i(t))$ is a differentiable and convex function concerning $x_i(t)$, the system (10) is deemed to be uniformly asymptotically stable at $x_e = 0$.

3 Synchronization of discrete incommensurate fractional-order neural networks

In the following analysis, we investigate the synchronization of incommensurate discrete fractional-order neural networks, characterized by

$$ {}^{C}\nabla_{a}^{\overline{\theta}} x(t) = -Cx(t) + Bf(t, x(t)). \tag{13}$$

In the provided equation, $\mathfrak{i}$ belongs to the set of natural numbers $\mathbb{N} = 1, 2, \ldots, n$, with t being greater than or equal to zero. The parameter $\overline{\theta} = [\theta_1, \theta_2, \ldots, \theta_n]$ denotes the vector of orders, where n represents the total number of units in the neural network. At time t, the state vector $x(t) = (x_1(t), \ldots, x_n(t))^T$ lies in $\mathbb{R}^n$, and $f(x(t)) = (f_1(x_1(t)), \ldots, f_n(x_n(t)))^T$ signifies the activation function of the neurons. Additionally, $C = \text{diag}(c_1, \ldots, c_n)$ signifies the diagonal matrix containing the constant rates at which each unit resets its potential individually, unaffected by external inputs or network activity. The weights governing the connection between the jth and $\mathfrak{i}$th neurons at time t are represented by $(a_{\mathfrak{i}j})n \times n$, and $I = (I_1, I_2, \ldots, In)^T$ denotes the external bias vector.

Before proceeding further, we state the following hypothesis:

(H_1): The activation functions f_j in the neural network exhibit Lipschitz continuity, ensuring the existence of positive constants l_j, where $j = 1, 2, \ldots, n$. These constants are defined such that

$$|f_j(x) - f_j(y)| < l_j|x - y|, \quad \text{for all } x, y \in \mathbb{R}.$$

The system denoted as (13) serves as the driving system, while the slave system is defined by

$$^C\nabla_a^{\overline{\theta}} y(t) = -Cy(t) + Bf(t, y(t)) + u(t). \tag{14}$$

Here, $y(t) \in \mathbb{R}^n$ represents the state vector of the slave system, with $u(t)$ representing the controller yet to be devised.

The discrepancy in states between the master and slave systems defines the synchronization error, articulated as

$$\mathfrak{e}(t) = y(t) - x(t). \tag{15}$$

The error dynamics, deduced from (13) to (14), can be expressed in the following manner:

$$^C\nabla_a^{\overline{\theta}} \mathfrak{e}(t) = -C\mathfrak{e}(t) + B(f(t, x(t)) - f(t, y(t))) + u(t). \tag{16}$$

Our objective is to devise an appropriate feedback control strategy,

$$u(t) = K\mathfrak{e}(t), \tag{17}$$

where $\mathbf{K} = \text{diag}(\kappa_1, \kappa_2, \ldots, \kappa_n)$ is a diagonal matrix, such that the subsequent error system takes the form:

$$^C\nabla_a^{\overline{\theta}} \mathfrak{e}(t) = -(C - K)\mathfrak{e}(t) + B(f(t, x(t)) - f(t, y(t))). \tag{18}$$

Alternatively,

$$ {}^{C}\nabla_{a}^{\theta_{\mathrm{i}}}\mathfrak{e}_{\mathrm{i}}(t) = -(c_{\mathrm{i}} - k_{\mathrm{i}})\mathfrak{e}_{\mathrm{i}}(t) + \sum_{j=1}^{n} b_{\mathrm{i}j}(f_j(t, x_j(t)) - f_j(t, y_j(t))), \quad i = 1, 2, \ldots, n. \tag{19} $$

The asymptotic stability implies that the trajectory of the slave system governed by (14) tends towards the trajectory of the master system over time, initialized at $y(a)$, and has the capability to gradually converge towards the drive system defined by (13), initiated at $x(a)$

$$ \lim_{t\to\infty} \|\mathfrak{e}(t)\| = \lim_{t\to\infty} \|x(t) - y(t)\| = 0. \tag{20} $$

Theorem 3.1. If (H_1) is valid, and the subsequent condition is met:

$$ k_{\mathrm{i}} > c_{\mathrm{i}} - \sum_{j=1}^{n} \frac{|b_{\mathrm{i}j}|l_j + |b_{j\mathrm{i}}|l_{\mathrm{i}}}{2}, \tag{21} $$

then the master-slave systems (13)-(14) achieve synchronization.

Proof. Choose the auxiliary function:

$$ V(t) = \sum_{\mathrm{i}=1}^{n} V_{\mathrm{i}}(t) = \frac{1}{2}\sum_{\mathrm{i}=1}^{n} \mathfrak{e}_{\mathrm{i}}^2(t). \tag{22} $$

Employing Lemma 2.2 and computing the θ_i-order difference on $\mathcal{V}_i$, we derive

$$ \begin{aligned} {}^{C}\nabla_{a}^{\theta_{\mathrm{i}}} V_{\mathrm{i}}(t) &\le \mathfrak{e}_{\mathrm{i}}(t)\, {}^{C}\nabla_{a}^{\theta_{\mathrm{i}}}\mathfrak{e}_{\mathrm{i}}(t), \\ &= \mathfrak{e}_{\mathrm{i}}(t)\left(-(c_{\mathrm{i}} - k_{\mathrm{i}})\mathfrak{e}_{\mathrm{i}}(t) + \sum_{j=1}^{n} b_{\mathrm{i}j}(f_j(t, x_j(t)) - f_j(t, y_j(t)))\right) \\ &\le -(c_{\mathrm{i}} - k_1)\mathfrak{e}_{\mathrm{i}}^2(t) + \sum_{j=1}^{n} |b_{\mathrm{i}j}| l_j \mathfrak{e}_{\mathrm{i}}(t)\mathfrak{e}_j(t) \\ &\le -(c_{\mathrm{i}} - k_{\mathrm{i}})\mathfrak{e}_{\mathrm{i}}^2(t) + \sum_{j=1}^{n} |b_{\mathrm{i}j}| l_j \frac{\mathfrak{e}_{\mathrm{i}}^2(t) + \mathfrak{e}_j^2(t)}{2} \\ &\le -(c_{\mathrm{i}} - k_{\mathrm{i}})\mathfrak{e}_{\mathrm{i}}^2(t) + \mathfrak{e}_{\mathrm{i}}^2(t)\sum_{j=1}^{n} \frac{|b_{\mathrm{i}j}|l_j + |b_{j\mathrm{i}}|l_{\mathrm{i}}}{2} \\ &\le -\left(c_{\mathrm{i}} - k_{\mathrm{i}} - \sum_{j=1}^{n} \frac{|b_{\mathrm{i}j}|l_j + |b_{j\mathrm{i}}|l_1}{2}\right)\mathfrak{e}_{\mathrm{i}}^2(t) \\ &= -\left(c_{\mathrm{i}} - k_{\mathrm{i}} - \sum_{j=1}^{n} \frac{|b_{\mathrm{i}j}|l_j + |b_{j\mathrm{i}}|l_{\mathrm{i}}}{2}\right) V_{\mathrm{i}}(t). \end{aligned} \tag{23} $$

Utilizing (23), we can formulate the corresponding comparative system:

$$\begin{bmatrix} {}^{C}\nabla_a^{\theta_1} W_1(t) \\ {}^{C}\nabla_a^{\theta_2} W_2(t) \\ \vdots \\ {}^{C}\nabla_a^{\theta_n} W_n(t) \end{bmatrix} = \begin{bmatrix} \epsilon_{11} & 0 & \cdots & 0 \\ 0 & \epsilon_{22} & \cdots & 0 \\ \vdots & \vdots & \ddots & \vdots \\ 0 & 0 & \cdots & \epsilon_{nn} \end{bmatrix} \begin{bmatrix} W_1(t) \\ W_2(t) \\ \vdots \\ W_n(t) \end{bmatrix}, \tag{24}$$

in which

$$\epsilon_{\mathrm{ii}} = -\left(c_{\mathrm{i}} - k_{\mathrm{i}} - \sum_{j=1}^{n} \frac{|b_{\mathrm{i}j}| l_j + |b_{j\mathrm{i}}| l_{\mathrm{i}}}{2} \right). \tag{25}$$

The system represented by (24) can be reformulated as

$$ {}^{C}\nabla_a^{\overline{\theta}} W(t) = AW(t). \tag{26}$$

Let $W(t) = (W_1(t), W_2(t), \ldots, W_n(t))^T$ and let $A = \mathrm{diag}\epsilon_{\mathrm{ii}} n \times n$. Lemma 2.1 implies that the controlled system (26) is asymptotically stable if a certain condition is met, specifically if $W(t) \to 0$ when $k_{\mathrm{i}} > c_{\mathrm{i}} - \sum j = 1^n \dfrac{|b_{\mathrm{i}j}| l_j + |b_{j\mathrm{i}}| l_{\mathrm{i}}}{2}$. By employing the comparison principle from Lemma 2.1, we deduce that $V(t) \leq W(t)$ and $V(t) \to 0$. Given $V(t) = \sum_{\mathrm{i}=1}^{n} V_{\mathrm{i}}(t) = \sum_{\mathrm{i}=1}^{n} \mathfrak{e}_{\mathrm{i}}^2(t)$, it follows that $\mathfrak{e}_{\mathrm{i}}(t) \to 0$. Consequently, the synchronization error system (16) is also stable, thus concluding the proof.

□

4 Synchronization of incommensurate discrete variable-order neural network

Let us explore the synchronization of a discrete incommensurate variable-order neural network, denoted by (27). We introduce an innovative theorem to ensure synchronized dynamics between two chaotic neural networks using simple linear control laws. Consider the discrete incommensurate variable-order neural network defined by (27) as the master system:

$$\begin{cases} {}^{C}\nabla_a^{\theta_1(t)} x_1(t) = -c_1 x_1(t) + \sum_{j=1}^{n} b_{\mathrm{i}j} f_j(t, x_j(t)), \\ {}^{C}\nabla_a^{\theta_2(t)} x_2(t) = -c_2 x_2(t) + \sum_{j=1}^{n} b_{2j} f_j(t, x_j(t)), \\ \vdots \\ {}^{C}\nabla_a^{\theta_n(t)} x_n(t) = -c_n x_n(t) + \sum_{j=1}^{n} b_{nj} f_j(t, x_j(t)). \end{cases} \tag{27}$$

Conversely, the controlled discrete incommensurate variable-order neural network represented by (28) is regarded as the slave system, with n synchronization controllers denoted as $L_1, L_2, \ldots, L_n$, respectively:

$$\begin{cases} {}^C\nabla_a^{\theta_1(t)} y_1(t) = -c_1 y_1(t) + \sum_{j=1}^n b_{\mathfrak{i}j} f_j(t, y_j(t)) + L_1(t), \\ {}^C\nabla_a^{\theta_2(t)} y_2(t) = -c_2 y_2(t) + \sum_{j=1}^n b_{2j} f_j(t, y_j(t)) + L_2(t), \\ \vdots \\ {}^C\nabla_a^{\theta_n(t)} y_n(t) = -c_n y_n(t) + \sum_{j=1}^n b_{nj} f_j(t, y_j(t)) + L_n(t). \end{cases} \tag{28}$$

To achieve complete synchronization, the synchronization error is defined as follows:

$$\mathfrak{e}_\mathfrak{i}(t) = x_\mathfrak{i}(t) - y_\mathfrak{i}(t), \quad i = 1, \ldots, n. \tag{29}$$

The synchronization scheme is deemed successful if the following condition holds:

$$\lim_{s \to +\infty} |\mathfrak{e}_\mathfrak{i}(t)| = 0, \qquad \text{for } \mathfrak{i} = 1, \ldots, n. \tag{30}$$

In order to emphasize the pivotal results of the proposed synchronization strategy, the ensuing theorem is introduced to guarantee the synchronization between the master and slave neural networks.

Theorem 4.1. The master-slave systems represented by (27) and (28) achieve synchronization when the controlled variables $L\mathfrak{i}, \mathfrak{i} = 1, \ldots, n$, are chosen as follows:

$$L_\mathfrak{i}(t) = -\left(\sum_{j=1}^n \frac{|b_{\mathfrak{i}j}| l_j + |b_{j\mathfrak{i}}| l_\mathfrak{i}}{2} \right) \mathfrak{e}_\mathfrak{i}(t), \quad \mathfrak{i} = 1, \ldots, n. \tag{31}$$

Proof. To ensure the convergence of the synchronization errors defined in (29), we begin by applying the nabla Caputo-type variable-order differences to (29), resulting in

$$\begin{cases} {}^C\nabla_a^{\theta_1(t)} e_1(t) &= -c_1 \mathfrak{e}_1(t) + \sum_{j=1}^n b_{1j}(f_j(t, x_j(t)) - f_j(t, y_j(t))) + L_1(t), \\ {}^C\nabla_a^{\theta_2(t)} e_2(t) &= -c_2 \mathfrak{e}_2(t) + \sum_{j=1}^n b_{2j}(f_j(t, x_j(t)) - f_j(t, y_j(t))) + L_2(t), \\ &\vdots \\ {}^C\nabla_a^{\theta_n(t)} e_n(t) &= -c_n \mathfrak{e}_n(t) + \sum_{j=1}^n b_{nj}(f_j(t, x_j(t)) - f_j(t, y_j(t))) + L_n(t). \end{cases} \tag{32}$$

Substituting the proposed control law (31) for $L_\mathfrak{i}, \mathfrak{i} = 1, \ldots, n$, in system (32) yields the following updated fractional discrete system:

$$\begin{cases} {}^C\nabla_a^{\theta_1(t)}\mathfrak{e}_1(t) = & -c_1\mathfrak{e}_1(t) + \sum_{j=1}^n b_{nj}(f_j(t,x_j(t)) - f_j(t,y_j(t))) \\ & - \left(\sum_{j=1}^n \dfrac{|b_{1j}|l_j + |b_{j1}|l_1}{2}\right)\mathfrak{e}_1(t), \\ {}^C\nabla_a^{\theta_2(t)}\mathfrak{e}_2(t) = & -c_2\mathfrak{e}_2(t) + \sum_{j=1}^n b_{nj}(f_j(t,x_j(t)) - f_j(t,y_j(t))) \\ & - \left(\sum_{j=1}^n \dfrac{|b_{2j}|l_j + |b_{j2}|l_2}{2}\right)\mathfrak{e}_2(t), \\ & \vdots \\ {}^C\nabla_a^{\theta_n(t)}\mathfrak{e}_n(t) = & -c_n\mathfrak{e}_n(t) + \sum_{j=1}^n b_{nj}(f_j(t,x_j(t)) - f_j(t,y_j(t))) \\ & - \left(\sum_{j=1}^n \dfrac{|b_{nj}|l_j + |b_{jn}|l_n}{2}\right)\mathfrak{e}_n(t). \end{cases} \tag{33}$$

We proceed to examine the Lyapunov function, which incorporates the collective error state

$$V(t) = \frac{1}{2}\sum_{\mathrm{i}=1}^n {}^C\nabla_a^{\theta_\mathrm{i}(t)-\gamma} e\mathrm{i}^2(t). \tag{34}$$

This results in ${}^C\nabla_a^\gamma V(t) = \dfrac{1}{2}\sum_{\mathrm{i}=1}^n {}^C\nabla_a^{\theta_\mathrm{i}(t)} e_\mathrm{i}^2(t)$. Furthermore, utilizing Lemma 2.2, we derive the following inequality:

$$\begin{aligned} {}^C\nabla_a^\gamma V(t) &\le \sum_{\mathrm{i}=1}^n e_\mathrm{i}(t)\, {}^C\nabla_a^{\theta_\mathrm{i}(t)} e_\mathrm{i}(t) \\ &= \sum_{\mathrm{i}=1}^n e_\mathrm{i}(t)\left(-c_\mathrm{i}\mathfrak{e}_\mathrm{i}(t) + \sum_{j=1}^n b_{\mathrm{i}j}(f_j(t,x_j(t)) - f_j(t,y_j(t)))\right. \\ &\quad \left. - \left(\sum_{j=1}^n \frac{|b_{\mathrm{i}j}|l_j + |b_{j\mathrm{i}}|l_\mathrm{i}}{2}\right)\mathfrak{e}_\mathrm{i}(t)\right) \\ &\le \sum_{\mathrm{i}=1}^n -c_\mathrm{i}\mathfrak{e}_\mathrm{i}^2(t) + \sum_{j=1}^n |b_{\mathrm{i}j}|\mathfrak{e}_\mathrm{i}(t)\mathfrak{e}_j(t) - \left(\sum_{j=1}^n \frac{|b_{\mathrm{i}j}|l_j + |b_{j\mathrm{i}}|l_\mathrm{i}}{2}\right)\mathfrak{e}_\mathrm{i}^2(t) \\ &\le \sum_{\mathrm{i}=1}^n -c_\mathrm{i}\mathfrak{e}_\mathrm{i}^2(t) + \sum_{j=1}^n |b_{\mathrm{i}j}|\frac{\mathfrak{e}_\mathrm{i}^2(t) + \mathfrak{e}_j^2(t)}{2} - \left(\sum_{j=1}^n \frac{|b_{\mathrm{i}j}|l_j + |b_{j\mathrm{i}}|l_\mathrm{i}}{2}\right)\mathfrak{e}_\mathrm{i}^2(t) \\ &\le -\sum_{\mathrm{i}=1}^n c_\mathrm{i}\mathfrak{e}_\mathrm{i}^2(t) \le -\gamma\sum_{\mathrm{i}=1}^n \mathfrak{e}_\mathrm{i}^2(t) = -\gamma\|e(t)\| < 0. \end{aligned} \tag{35}$$

Additionally, based on Theorem 2.2, it can be affirmed that the dynamics of the error system (29) for discrete incommensurate variable-order networks converge towards zero, indicating stability. Consequently, the synchronization between the master system (27) and the slave system (28) of the discrete incommensurate variable-order neural network is successfully attained through the utilization of linear control laws (31). Thus, the proof is duly concluded. □

5 Numerical examples

In this section, we employ numerical simulations conducted in MATLAB to provide a comprehensive validation of the theoretical findings presented in the preceding theorem. Through detailed numerical experiments, we aim to offer a deeper understanding and insight into the synchronization behavior predicted by our theoretical framework.

Example 1. The master system is the incommensurate discrete fractional neural network with two neurons:

$$\begin{cases} {}^{C}\nabla_{a}^{\theta_1} x_1(t) &= -0.25x_1(t) + 0.1\sin(x_1(t)) - 0.2\sin(x_2(t)), \\ {}^{C}\nabla_{a}^{\theta_2} x_2(t) &= -0.3x_2(t) + 0.3\sin(x_1(t)) + 0.4\sin(x_2(t)). \end{cases} \tag{36}$$

The slave system is

$$\begin{cases} {}^{C}\nabla_{a}^{\theta_1} y_1(t) &= -1y_1(t) + 0.1\sin(y_1(t)) - 0.2\sin(y_2(t)) + k_1(t), \\ {}^{C}\nabla_{a}^{\theta_2} y_2(t) &= -1.5y_2(t) + 0.3\sin(y_1(t)) + 0.4\sin(y_2(t)) + k_2(t). \end{cases} \tag{37}$$

The synchronization state-feedback gain is determined as follows:

$$K = \begin{bmatrix} 0.2 & 0 \\ 0 & 0.1 \end{bmatrix}, \tag{38}$$

resulting in the matrix A defined as

$$A = \begin{bmatrix} 0.1 & 0 \\ 0 & 0.2 \end{bmatrix}. \tag{39}$$

Certainly, the matrix A fulfills the criteria delineated in both Theorem 2.1 and Theorem 2.2, signifying the asymptotic stability of the error system. This indicates the attainment of synchronization between the driving and responding systems. In our computational trials, we commence with the driving and responding systems initialized at $x(0) = (3, 1, 2)^T$ and $y(0) = (4, 2, 3)^T$, respectively. Figure 1 visually presents the evolution of state synchronization between these systems, while Figure 2 depicts the synchronization error.

Example 2. Let us regard the three-dimensional discrete incommensurate variable-order neural network expressed by (40) and (41) as the master-slave systems for our investigation:

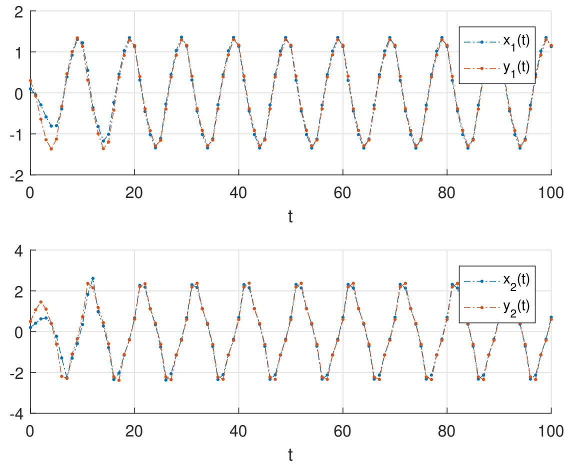

Figure 1: State trajectory of master-slave system (36)–(37).

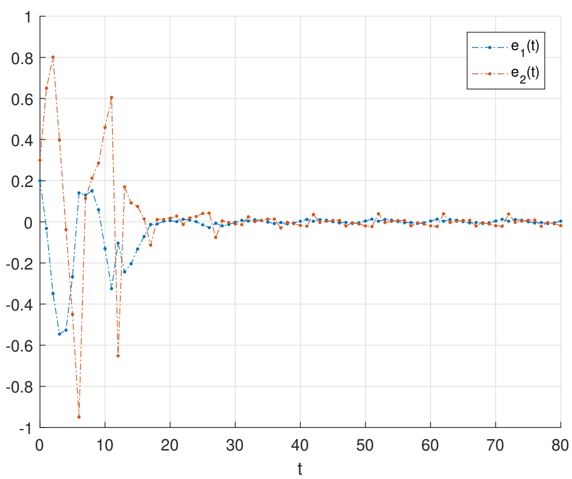

Figure 2: Time evolution of the error system.

$$\begin{cases} {}^{C}\nabla_a^{\theta_1(t)} x_1(t) = & -x_1(t) - 0.5\tanh(x_1(t)) - 0.7\tanh(x_2(t)) \\ & -0.5\tanh(x_3(t)), \\ {}^{C}\nabla_a^{\theta_2(t)} x_2(t) = & -x_2(t) - 0.6\tanh(x_1(t)) - \tanh(x_2(t)) \\ & +0.1\tanh(x_3(t)), \\ {}^{C}\nabla_a^{\theta_3(t)} x_3(t) = & -1.3x_3(t) - 0.6\tanh(x_1(t)) + 0.5\tanh(x_2(t)) \\ & -0.3\tanh(x_3(t)), \end{cases} \tag{40}$$

while,

$$\begin{cases} {}^C\nabla_a^{\theta_1(t)} y_1(t) = & -y_1(t) - 0.5\tanh(y_1(t)) - 0.7\tanh(y_2(t)) \\ & -0.5\tanh(y_3(t)) + L_1(t), \\ {}^C\nabla_a^{\theta_2(t)} y_2(t) = & -y_2(t) - 0.6\tanh(y_1(t)) - \tanh(y_2(t)) \\ & +0.1\tanh(y_3(t)) + L_2(t), \\ {}^C\nabla_a^{\theta_3(t)} y_3(t) = & -1.3y_3(t) - 0.6\tanh(y_1(t)) + 0.5\tanh(y_2(t)) \\ & -0.3\tanh(y_3(t)) + L_3(t). \end{cases} \tag{41}$$

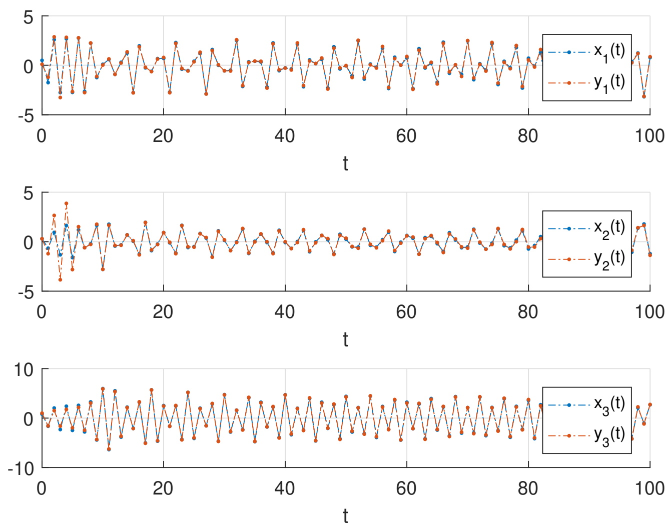

Figure 3: Trajectory of states in the master-slave systems (40)–(41).

The initial states, $\mathfrak{e}_1(0)$, $\mathfrak{e}_2(0)$, and $\mathfrak{e}_3(0)$, are considered as the starting values. To simulate the states of the variable-order error system and synchronized systems (40) and (41), the predictor-corrector method is employed. The initial values are specified as $x(0) = (0.5, 0.3, 0.8)^T$ and $y(0) = (0.1, 0.3, 1)^T$ with

$$\begin{cases} \theta_1(t) = \left|\dfrac{1}{2} - e^{-4(t+1)}\right|, \\ \theta_2(t) = \dfrac{1}{5}|\log(t+3)|, \\ \theta_3(t) = \dfrac{1}{2} - \dfrac{e^{\frac{-10}{t+1}}}{t+1}. \end{cases} \tag{42}$$

In Figure 3, the numerical states of the discrete incommensurate systems (40)–(41) are depicted. Meanwhile, Figure 4 illustrates the time evolution of the error system. These visualizations

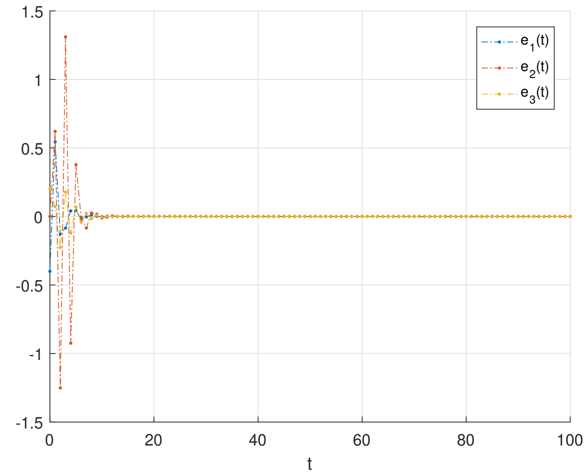

Figure 4: Temporal evolution of the error system.

distinctly demonstrate the synchronized dynamics achieved by the two chaotic fractional neural networks, confirming the effectiveness and simplicity of the linear control laws (31) in achieving synchronization.

6 Conclusion

In conclusion, this study has addressed the synchronization of incommensurate discrete fractional neural networks, which extends previous research focused on commensurate systems. By utilizing linear feedback control methods and establishing sufficient conditions for synchronization in terms of linear matrix inequalities, we provided a systematic approach applicable to networks with both constant and variable orders. The application of the Lyapunov functional under specific conditions further strengthened our analysis, offering insights into synchronization dynamics and facilitating easy verification and implementation. Through numerical examples, we demonstrated the effectiveness and feasibility of our proposed methods, underscoring their potential for practical applications in various fields reliant on network synchronization. Overall, our contributions advance the understanding and practical implementation of synchronization mechanisms in complex fractional-order neural networks.

Funding

This research received no external funding.

Conflicts of Interest

The authors declare no conflicts of interest.

References

[1] Abbes, A., Ouannas, A., Shawagfeh, N. and Khennaoui, A.A. *Incommensurate fractional discrete neural network: chaos and complexity*, Eur. Phys. J. Plus, 137(2) (2022), 235.

[2] Abdeljawad, T. *Dual identities in fractional difference calculus within Riemann*, Adv. Differ. Equ., 2013 (2013), 1–16.

[3] Almatroud, O.A., Hioual, A., Ouannas, A., Sawalha, M.M., Alshammari, S. and Alshammari, M. *On variable-order fractional discrete neural networks: existence, uniqueness and stability*, Fractal Fract., 7(2) (2023), 118.

[4] Azar, A.T., Vaidyanathan, S. and Ouannas, A. (Eds.). *Fractional order control and synchronization of chaotic systems* (Vol. 688). Springer, 2017.

[5] Chen, L., Yin, H., Huang, T., Yuan, L., Zheng, S. and Yin, L. *Chaos in fractional-order discrete neural networks with application to image encryption*, Neural Netw., 125 (2020), 174–184.

[6] Cui, X., Li, H.L., Zhang, L., Hu, C. and Bao, H. *Complete synchronization for discrete-time fractional-order coupled neural networks with time delays*, Chaos Solitons Fractals, 174 (2023), 113772.

[7] Djenina, N., Ouannas, A., Oussaeif, T.E., Grassi, G., Batiha, I.M., Momani, S. and Albadarneh, R.B. *On the stability of incommensurate h-nabla fractional-order difference systems*, Fractal Fract., 6(3) (2022), 158.

[8] Djennoune, S., Bettayeb, M. and Al-Saggaf, U.M. *Synchronization of fractional-order discrete-time chaotic systems by an exact delayed state reconstructor: Application to secure communication*, Int. J. Appl. Math. Comput. Sci., 29(1) (2019), 179–194.

[9] Gu, Y., Wang, H. and Yu, Y. *Synchronization for incommensurate Riemann–Liouville fractional-order time-delayed competitive neural networks with different time scales and known or unknown parameters*, J. Comput. Nonlinear Dyn., 14(5) (2019), 051002.

[10] Gu, Y., Wang, H. and Yu, Y. *Synchronization for fractional-order discrete-time neural networks with time delays*, Appl. Math. Comput., 372 (2020), 124995.

[11] Hamadneh, T., Hioual, A., Alsayyed, O., Al-Khassawneh, Y.A., Al-Husban, A. and Ouannas, A. *Finite Time Stability Results for Neural Networks Described by Variable-Order Fractional Difference Equations*, Fractal Fract., 7(8) (2023), 616.

[12] Hein, J., McCarthy, Z., Gaswick, N., McKain, B. and Speer, K. *Laplace transforms for the nabla-difference operator*, Pan Am. Math. J., 21(3) (2011), 79–96.

[13] Hioual, A., Ouannas, A., Grassi, G. and Oussaeif, T.E. *Nonlinear nabla variable-order fractional discrete systems: Asymptotic stability and application to neural networks*, J. Comput. Appl. Math., 423 (2023), 114939.

[14] Hioual, A., Ouannas, A., Momani, S. and Oussaeif, T.E. *Finite-Time Stability of ABC Type h-Fractional Discrete Neural Networks: Gronwall Inequality and Stability Criterion*, In *2023 International Conference on Fractional Differentiation and Its Applications (ICFDA)*, pp. 1–6. IEEE, 2023.

[15] Hioual, A., Ouannas, A. and Oussaeif, T.E. *Nonlinear Fractional Discrete Neural Networks: Stability, Stabilization and Synchronization*, In *State Estimation and Stabilization of Nonlinear Systems: Theory and Applications*, pp. 169–204. Springer Nature Switzerland, Cham, 2023.

[16] Hioual, A., Ouannas, A., Oussaeif, T.E., Grassi, G., Batiha, I.M. and Momani, S. *On variable-order fractional discrete neural networks: solvability and stability*, Fractal Fract., 6(2) (2022), 119.

[17] Hioual, A., Oussaeif, T.E., Ouannas, A., Grassi, G., Batiha, I.M. and Momani, S. *New results for the stability of fractional-order discrete-time neural networks*, Alex. Eng. J., 61(12) (2022), 10359–10369.

[18] Jia, J., Wang, F. and Zeng, Z. *Lag quasi-synchronization of incommensurate fractional-order memristor-based neural networks with nonidentical characteristics via quantized control: A vector fractional Halanay inequality approach*, J. Franklin Inst., 359(12) (2022), 6392–6437.

[19] Khennaoui, A.A., Ouannas, A., Bendoukha, S., Grassi, G., Lozi, R.P. and Pham, V.T. *On fractional-order discrete-time systems: Chaos, stabilization and synchronization*, Chaos Solitons Fractals, 119 (2019), 150–162.

[20] Kuang, Z., Gao, H. and Tomizuka, M. *Precise linear-motor synchronization control via cross-coupled second-order discrete-time fractional-order sliding mode*, IEEE/ASME Trans. Mechatronics, 26(1) (2020), 358–368.

[21] Li, X., Fang, J.A., Zhang, W. and Li, H. *Finite-time synchronization of fractional-order memristive recurrent neural networks with discontinuous activation functions*, Neurocomputing, 316 (2018), 284–293.

[22] Liu, X. and Yu, Y. *Synchronization analysis for discrete fractional-order complex-valued neural networks with time delays*, Neural Comput. Appl., 33 (2021), 10503–10514.

[23] Megherbi, O., Hamiche, H., Djennoune, S. and Bettayeb, M. *A new contribution for the impulsive synchronization of fractional-order discrete-time chaotic systems*, Nonlinear Dyn., 90 (2017), 1519–1533.

[24] Momani, S., Batiha, I.M., Hioual, A. and Ouannas, A. *Fractional Neural Networks: Finite time stability and its application to synchronization*, In *2023 International Conference on Fractional Differentiation and Its Applications (ICFDA)*, pp. 1–5. IEEE, 2023.

[25] Ouannas, A., Azar, A.T. and Abu-Saris, R. *A new type of hybrid synchronization between arbitrary hyperchaotic maps*, Int. J. Mach. Learn. Cybern., 8(6) (2017), 1887–1894.

[26] Ouannas, A., Azar, A.T. and Vaidyanathan, S. *A robust method for new fractional hybrid chaos synchronization*, Math. Methods Appl. Sci., 40(5) (2017), 1804–1812.

[27] Ouannas, A., Azar, A.T. and Vaidyanathan, S. *New hybrid synchronisation schemes based on coexistence of various types of synchronisation between master-slave hyperchaotic systems*, Int. J. Comput. Appl. Technol., 55(2) (2017), 112–120.

[28] Ouannas, A., Azar, A.T. and Ziar, T. *On inverse full state hybrid function projective synchronization for continuous-time chaotic dynamical systems with arbitrary dimensions*, Differ. Equ. Dyn. Syst., 28(4) (2020), 1045–1058.

[29] Ouannas, A., Azar, A.T., Ziar, T. and Radwan, A.G. *Generalized synchronization of different dimensional integer-order and fractional order chaotic systems*, In *Fractional Order Control and Synchronization of Chaotic Systems*, pp. 671–697. Springer, Cham, 2017.

[30] Ouannas, A., Karouma, A., Grassi, G., Pham, V.T. and Luong, V.S. *A novel secure communications scheme based on chaotic modulation, recursive encryption and chaotic masking*, Alex. Eng. J., 60(1) (2021), 1873–1884.

[31] Ouannas, A., Khennaoui, A.A., Momani, S., Grassi, G. and Pham, V.T. *Chaos and control of a three-dimensional fractional order discrete-time system with no equilibrium and its synchronization*, AIP Adv., 10(4) (2020).

[32] Ouannas, A. and Odibat, Z. *Generalized synchronization of different dimensional chaotic dynamical systems in discrete time*, Nonlinear Dyn., 81(1) (2015), 765–771.

[33] Si, L., Xiao, M., Jiang, G., Cheng, Z., Song, Q. and Cao, J. *Dynamics of fractional-order neural networks with discrete and distributed delays*, IEEE Access, 8 (2019), 46071–46080.

[34] Wang, M., Wang, Y. and Chu, R. *Dynamical Analysis of the Incommensurate Fractional-Order Hopfield Neural Network System and Its Digital Circuit Realization*, Fractal Fract., 7(6) (2023), 474.

[35] Wang, S. and Jian, J. *Predefined-time synchronization of incommensurate fractional-order competitive neural networks with time-varying delays*, Chaos Solitons Fractals, 177 (2023), 114216.

[36] Xin, B. and Wu, Z. *Projective synchronization of chaotic discrete dynamical systems via linear state error feedback control*, Entropy, 17(5) (2015), 2677–2687.

[37] You, X., Song, Q. and Zhao, Z. *Global Mittag-Leffler stability and synchronization of discrete-time fractional-order complex-valued neural networks with time delay*, Neural Netw., 122 (2020), 382–394.

[38] Zhao, M., Li, H.L., Zhang, L., Hu, C. and Jiang, H. *Quasi-projective synchronization of discrete-time fractional-order quaternion-valued neural networks*, J. Franklin Inst., 360(4) (2023), 3263–3279.